

Single-nucleotide polymorphism screening and RNA sequencing of key messenger RNAs associated with neonatal hypoxic-ischemia brain damage

Liu-Lin Xiong^{1,2,#}, Lu-Lu Xue^{3,#}, Mohammed Al-Hawwas², Jin Huang³, Rui-Ze Niu³, Ya-Xin Tan³, Yang Xu⁴, Ying-Ying Su⁴, Jia Liu^{3,*}, Ting-Hua Wang^{3,4,*}

1 Department of Anesthesiology, National Traditional Chinese Medicine Clinical Research Base and Western Medicine Translational Medicine Research Center, Affiliated Traditional Chinese Medicine Hospital, Southwest Medical University, Luzhou, Sichuan Province, China

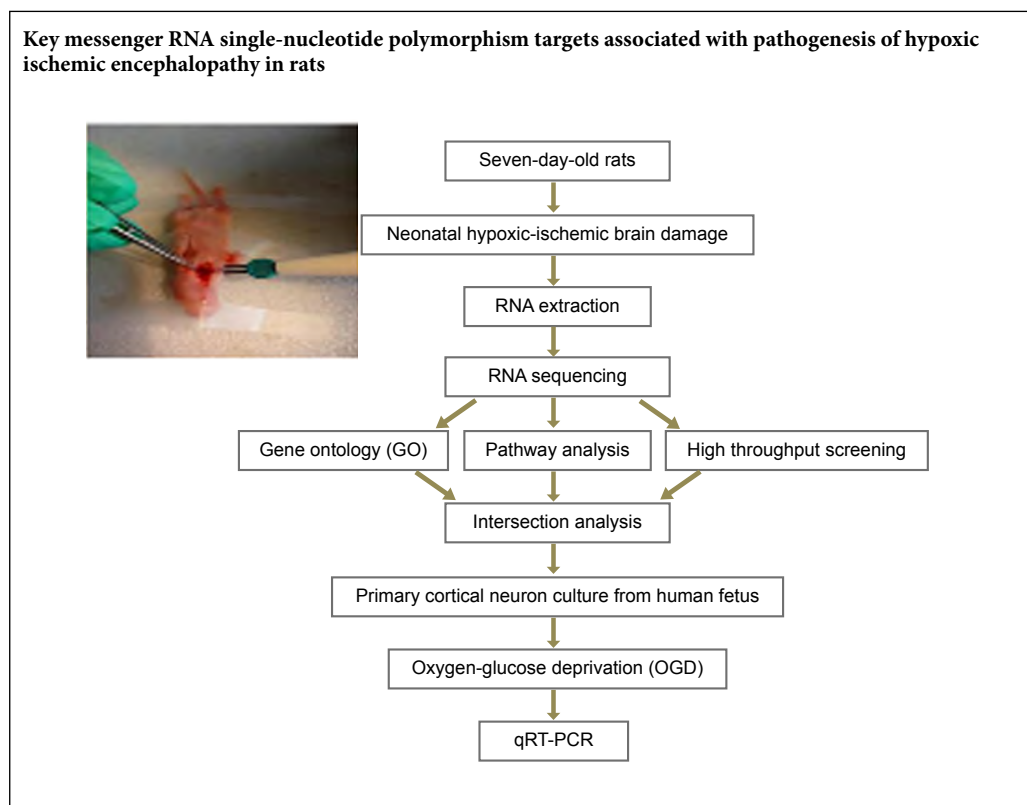
2 School of Pharmacy and Medical Sciences, Division of Health Sciences, University of South Australia, Adelaide, South Australia, Australia

3 Department of Animal Zoology, Kunming Medical University, Kunming, Yunnan Province, China

4 Institute of Neurological Disease, Department of Anesthesiology, Translational Neuroscience Center, West China Hospital, Sichuan University, Chengdu, Sichuan Province, China

Funding: This study was supported by the program Innovative Research Team in Science and Technology in Yunnan Province of China (to THW); the National Natural Science Foundation of China, No. 81601074, Sichuan Provincial Scientific Foundation Grant of China, No. 2017SZ0145.

Graphical Abstract



*Correspondence to:

Jia Liu, PhD,

liujiaaixuexi@126.com;

Ting-Hua Wang, PhD,

wangtinghua@vip.163.com.

#Both authors contributed equally to this work.

orcid:

0000-0003-2012-8936

(Ting-Hua Wang)

0000-0001-5678-7437

(Jia Liu)

doi: 10.4103/1673-5374.264469

Received: August 16, 2018

Accepted: April 24, 2019

Abstract

A single-nucleotide polymorphism (SNP) is an alteration in one nucleotide in a certain position within a genome. SNPs are associated with disease susceptibility. However, the influences of SNPs on the pathogenesis of neonatal hypoxic-ischemic brain damage remain elusive. Seven-day-old rats were used to establish a hypoxic ischemic encephalopathy model. SNPs and expression profiles of mRNAs were analyzed in hypoxic ischemic encephalopathy model rats using RNA sequencing. Genes exhibiting SNPs associated with hypoxic ischemic encephalopathy were identified and studied by gene ontology and pathway analysis to identify their possible involvement in the disease mechanism. We identified 89 up-regulated genes containing SNPs that were mainly located on chromosome 1 and 2. Gene ontology analysis indicated that the up-regulated genes containing SNPs are mainly involved in angiogenesis, wound healing and glutamatergic synapse and biological processing of calcium-activated chloride channels. Signaling pathway analysis indicated that the differentially expressed genes play a role in glutamatergic synapses, long-term depression and oxytocin signaling. Moreover, intersection analysis of high throughput screening following PubMed retrieval and RNA sequencing for SNPs showed that CSRN1, DUSP5 and LRRC25 were most relevant to hypoxic ischemic encephalopathy. Significant up-regulation of genes was confirmed by quantitative real-time polymerase chain reaction analysis of

oxygen-glucose-deprived human fetal cortical neurons. Our results indicate that *CSRN1*, *DUSP5* and *LRRC25*, containing SNPs, may be involved in the pathogenesis of hypoxic ischemic encephalopathy. These findings indicate a novel direction for further hypoxic ischemic encephalopathy research. This animal study was approved on February 5, 2017 by the Animal Care and Use Committee of Kunming Medical University, Yunnan Province, China (approval No. kmmu2019038). Cerebral tissue collection from a human fetus was approved on September 30, 2015 by the Ethics Committee of Kunming Medical University, China (approval No. 2015-9).

Key Words: *CSRN1*; *DUSP5*; gene ontology analysis; human fetal cortical neurons; *LRRC25*; mRNA; neonatal hypoxic ischemic encephalopathy; pathogenesis; signaling pathway analysis

Chinese Library Classification No. R446; R654.5+5; R741

Introduction

Hypoxic ischemic encephalopathy (HIE) refers to a serious neurological syndrome that occurs in the earliest days of life because of placental insufficiency or umbilical cord occlusion in the perinatal period (Allen and Brandon, 2011). HIE is a major neuro-developmental disability in infants, with a prevalence of approximately 1 to 6 per 1000 births (Vannucci, 2000; Chau et al., 2014). Twenty-five percent of HIE patients suffer permanent neurological deficits (Graham et al., 2008). Additionally, worldwide, approximately one million newborns die from HIE each year (Lv et al., 2017). HIE can result in periventricular leukomalacia or developmental retardation, and can cause dysfunction in remote organs (Zeppellini et al., 2001; Wu et al., 2011; Zhao et al., 2012; Alaro et al., 2014; Khatri et al., 2014; Saeed et al., 2014). Despite numerous clinical trials, many neuro-protective strategies have failed to effectively treat HIE patients. The need to expand our understanding of HIE mechanisms and to develop novel therapies is therefore urgent (Ginsberg, 2008; Davies et al., 2019).

A single-nucleotide polymorphism (SNP) is the substitution of a single nucleotide at a certain position in a genome. Generally, SNPs are present at varying percentages within a population (e.g., > 1%) and most do not cause any disorder. However, SNPs have been linked to disorders; for example SNPs in non-coding regions can increase the risk of cancer (Li et al., 2014) or they can influence messenger RNA (mRNA) structure to increase disease susceptibility (Lu et al., 2015). This is in addition to the well-characterized SNPs related to drug metabolism. Research into SNPs is therefore important to identify an individual's genetic tendency to develop particular diseases (Goldstein, 2001; Lee, 2004; Yanase et al., 2006; Li et al., 2019). SNPs in vasoactive intestinal polypeptide and N-methyl-D-aspartate receptor subunit 3A play roles in cerebral palsy in two-year-old infants after preterm birth (Costantine et al., 2012). Therefore, to observe the role of SNPs in HIE, we aimed to detect key SNPs associated with HIE pathogenesis in rats.

RNA sequencing (RNA-seq), also known as second-generation sequencing, is a powerful tool to analyze transcriptome changes within cells and tissues. This approach enables the collection of data on gene fusion and spliced transcripts, post-transcriptional modifications, gene expression over time and SNP diagnosis (Maher et al., 2009). It also distinguishes RNA populations, such as ribosomal RNAs, transfer RNAs, microRNAs and small RNAs (Ingolia et al., 2012). Recently, this technology has been widely used to investigate the differential expression of genes. Therefore, in the present study, we used RNA-Seq to identify SNPs and changes in gene expression in rats subjected to HIE. We sought to iden-

tify SNPs involved in HIE, with the eventual aim of evaluating the genetic predisposition of an individual to developing HIE.

We used seven-day-old rats to establish a HIE model. SNPs and the expression profiles of mRNAs were analyzed in HIE and control brains using RNA-seq and compared. Genes exhibiting SNPs associated with HIE were identified and studied by gene ontology (GO) and pathway analysis to identify their possible involvement in the disease mechanism.

Materials and Methods

Animal care and grouping

Animal experiments and animal handling procedures were approved on February 5, 2017 by the Animal Care and Use Committee of Kunming Medical University, Kunming, Yunnan Province, China (approval No. kmmu2019038) and were performed in accordance with the guidelines of the United States National Institutes of Health. Twenty-four specific pathogen-free one-week-old male Sprague-Dawley rats weighing 100–200 g were procured from the Animal Centre of Kunming Medical University (Yunnan, China) (license No. SCXK k2015-0002). The neonate rats were housed at 21–25°C and 45–50% humidity. The animals were exposed to light for 12 hours during the daytime with free access to food and water. Pups were randomly allocated to the sham-operated group (sham, $n = 12$) and the HIE group (HIE, $n = 12$). The HIE group was subjected to permanent hypoxia ischemia. The sham-operated group was reared under standard conditions (**Figure 1A & B**).

Induction of hypoxia-ischemia brain damage

HIE was induced using the suture occlusion technique as described previously (Ding et al., 2017). Briefly, animals were anesthetized using isoflurane and immobilized. A 0.5 cm skin incision was made along the midline of the neck, and the right common carotid artery was exposed and occluded with an electrocoagulator (Spring Medical Beauty Equipment Co., Wuhan, Hubei Province, China). Following the surgical procedure, the pups were returned to their dams for recovery and feeding for 1 hour. The pups were then placed into an airtight chamber maintained at 37°C and subjected to hypoxia for 2 hours (8% O₂, 92% N₂). The sham group underwent anesthesia and the common carotid artery was exposed but not ligated. The sham group was not exposed to hypoxia.

Measurement of body weight

Animals were weighed on a high precision balance (Shanghai puchun measure instrument Co., Shanghai, China) before surgery and at 24 hours after HIE.

Zea-longa neurological score

To evaluate the success of HIE model establishment and to identify behavioral changes following the operation, animals were assessed for neurological disorders before surgery and 0, 2, 4, 6, 12, 20 and 24 hours post-surgery. The Zea-longa neurological score was performed as described previously with minor modifications (Wang et al., 2010b). Zero points were given for normal behaviors and symmetric double forelimb stretching. The rats whose contralateral forelimb weakness, torso turning or ipsilateral hindlimb could not fully stretch scored 1 point. Affected posture and circling towards the injured side scored 2 points, while 3 point was given to animals that could not weight-bear on the affected side and 4 point indicated that animals could not weight-bear on the affected side and did not exhibit spontaneous locomotor activity or displayed barrel rolling. The animals in the model group with a score ≥ 1 were selected for further analysis.

High-throughput screening

High-throughput screening technologies were performed to search for the key factors participating in the occurrence and development of HIE. The standard as follow: 1) remove the genes reported in the Scientific Citation Index (SCI) paper on the functional and clinical relevance of the cancer species studied in this project; 2) removal of multiple transmembrane protein genes; 3) remove genes that are not explicitly annotated (such as with open reading frame); 4) remove the number of PubMed articles more than 60; 5) existing experimental data to filter genes combined with the key gene database of Kikekien disease.

RNA extraction

At 24 hours post-operation, pups were deeply anesthetized by intraperitoneal injection of pentobarbitone sodium (200–300 μ L; 30 mg/m), before perfusion with PBS (pH 7.4) through the heart. The brain cortex was then quickly dissected and placed on dry ice. Total RNA was extracted from the ipsilateral cortex using an RNeasy Mini Kit (Qiagen, Shanghai, China) in accordance with the manufacturer's protocol. Briefly, RNA from 12 HIE and 12 sham brain samples was pooled into two HIE and two sham pools, which were used for RNA-Seq analysis (performed by Bi-omarker Technologies Co., Beijing, China) (Rodríguez et al., 2014; Seeliger et al., 2014; Wang et al., 2016). Briefly, RNA integrity was confirmed by 2% agarose gel electrophoresis and by analysis on an Agilent Bioanalyzer 2100 System (Agilent Technologies, CA, USA). RNA concentrations were calculated using a NanoDrop 2000 Spectrophotometer (Thermo Fisher Scientific, Wilmington, DE, USA). Finally, ribosomal RNA was depleted in the samples with a Ribo-Zero Ribosomal RNA Removal Kit (Epicentre, Madison, WI, USA).

Construction of mRNA-seq libraries

Sequencing libraries were constructed using the NEBNext[®] Ultra[®] Directional RNA Library Prep Kit for Illumina[®] (NEB, New England, USA) according to the manufacturer's instructions by Biomarker Technologies Co. (Beijing, China). Briefly, mRNA was fragmented by heating to 94°C for 15 minutes in 5 \times NEBNext First Strand Synthesis Reaction

Buffer. Random primers, reverse transcriptase and murine RNase inhibitor were then added and first strand complementary DNA (cDNA) synthesized at 42°C for 30 minutes. Then, second-strand cDNA was synthesized using a synthesis enzyme mix for 60 minutes at 16°C then for 30 minutes at 20°C. The resulting dsDNA fragments were purified using Agencourt AMPure XP Beads (Beckman Coulter, Beverly, CA, USA). The overhangs were digested to blunt ends with NEB Next End Prep Enzyme Mix and then adaptors linked to the USER Enzyme were ligated to the cDNA. cDNA was then purified using AMPure XP Beads. Finally, the DNA fragments were amplified using Hot Start HiFi PCR Master Mix, and the products were re-purified using the AMPure XP system and library quality was analyzed using an Agilent Bioanalyzer 2100 and qRT-PCR.

Bioinformatic analysis and differential expression analysis

TruSeq PE Cluster Kitv3-cBot-HS was adopted to construct clusters of index-coded samples on an acBot Cluster Generation System (Illumina Inc., San Diego, CA, USA). The RNA library was then sequenced on an Illumina Hiseq platform and paired-end reads generated. The resultant raw reads were further cleaned by eliminating adapter sequences, low-quality reads and poly-N sequences. Furthermore, sequences below 20 nucleotides or more than 30 nucleotides were removed from the clean data to avoid any disruption to downstream analyses. The GC-content and sequence duplication levels of the clean data were then calculated to confirm the quality of the data.

Cufflinks package (version 2.1.1; <https://launchpad.net/ubuntu/+source/cufflinks>) was used to calculate expression of genes and lncRNAs depending on fragments per kilobase of exon per million reads (FPKM) values (Trapnell et al., 2010). DESeq R package (version 1.10.1) was used for statistical analysis of differential gene expression between groups. The *P* values were set to < 0.01 based on Benjamini and Hochberg's method to reduce the false discovery rate. Genes with a log₂ fold expression variation value > 1 were considered to be differentially expressed. EBseq was adopted for the samples without biological replicates (Storey and Tibshirani, 2003).

Gene functional annotation

The non-redundant protein sequence database of the National Center for Biotechnology Information, USA, was used to predict Gene function. Clusters of Orthologous Groups of proteins (KOG/COG) were used to study GO. GO R Packages for comprehensive study of gene function and variations were used to analyze differentially expressed genes and Pfams (Protein families). KEGG (Kyoto encyclopedia of genes and genomes) and KOBAS (KEGG orthology-based annotation system) were applied to identify the statistically enriched pathways of the differentially expressed genes (Mao et al., 2005). An intersection analysis was performed using Venny 2.1 (<http://bioinfogp.cnb.csic.es/tools/venny/>).

Primary culture of human fetal cortical neurons

Cerebral tissue collection from a 29-day-old human fetus was approved on September 30, 2015 by the Ethics Committee of Kunming Medical University, China (approval

No. 2015-9). Informed consent was obtained from the mother. An aborted 29 day-old fetus was collected from the first affiliated hospital of Kunming Medical University and immediately stored on ice. The brain was dissected and placed in 75% alcohol for 2 minutes. The cortical tissues were then harvested into cold Dulbecco's modified Eagle's medium (DMEM) and cut into 1 mm³ sized blocks. Trypsin (0.25%) digestion for 30 minutes at 37°C was then performed to isolate cells from the cortical tissue. Cells were then rinsed in DMEM containing 10% fetal bovine serum. The tissue suspension was centrifuged at 1000 × g for 10 minutes and the pelleted cells were then resuspended in complete culture medium (Hyclone, Logan, UT, USA) composed of DMEM/high glucose, 10% fetal calf serum and 1% penicillin-streptomycin solution. Neurons were plated in 6-well plates (Corning, New York, USA) coated with poly-D-lysine and laminin (Sigma-Aldrich, St. Louis, MO, USA) at a density of 5 × 10⁵ cells/mL, and incubated at 37°C in a 5% CO₂ atmosphere. Four hours later, the medium was replaced with neurobasal medium containing 2% B27 (Invitrogen, Carlsbad, CA, USA). The culture medium was changed the next day, then half the medium was changed every three days. The cells were then incubated with oxygen-glucose deprivation (OGD). Control group cells were not exposed to OGD.

In vitro OGD

In vitro human cortical neurons were prepared to mimic HIE using an OGD protocol (Joerger-Messerli et al., 2018). Briefly, cells were washed once with 0.01 mM PBS before the medium was changed to glucose-free medium. Cells were then transferred to a hypoxia chamber (Thermo Scientific, Waltham, MA, USA) and exposed to a gas mixture of 5%CO₂ and 95%N₂ for 2 hours. Control cells were incubated normally, without exposure to OGD.

Quantitative real-time polymerase chain reaction

Total RNA was isolated from human neurons 24 hours post OGD with Trizol reagent (Takara Bio Inc., Otsu, Japan). RNA was reverse transcribed to cDNA with the Revert Aid™ First Strand cDNA Synthesis kit (Thermo Scientific). qRT-PCR was then performed to detect the relative expression of mRNA according to previous protocols (Liu et al., 2014), with the primer sequences shown in **Table 1**. Reactions were performed in a DNA thermal cycler (Bio-Rad, Bole, USA) according to the following standard protocol: initial denaturation at 95°C for 2 minutes, denaturation at 95°C for 15 seconds, amplification at 53°C for 20 seconds, then at 60°C for 30 seconds for a total of 40 cycles. The threshold cycle (Ct) of each sample was recorded, and relative expression was calculated with normalization to β-actin values using the 2^{-ΔΔCt} method.

Statistical analysis

All data are expressed as the mean ± standard deviation (SD). Results were compared by Student's *t*-test using SPSS 17.0 (SPSS, Chicago, IL, USA). Multiple comparisons were adjusted by Benjamini-Hochberg. The *P* value was set at < 0.05.

Table 1 Primers used for quantitative real-time polymerase chain reaction

Gene	Sense	Antisense	Product size (bp)
LRRC25	5'-TAT CGG GGC AGT GGT C-3'	5'-CAT AGT CGG GAG TGG AGG G-3'	233
DUSP5	5'-GAG AAG ATT GAG AGT GAG A-3'	5'-ATC CAT TTG TAG TGT AGG T-3'	239
CSRNPI	5'-ATC CAC ACA CTC ACC CGC C-3'	5'-ATC CAC ACA CTC ACC CGC C-3'	193

Results

Establishment of a hypoxia-ischemia brain damage animal model

Rats were weighed before and after HIE surgery. The body-weight of the HIE rats was significantly reduced 24 hours post-surgery, whereas that of sham rats was not (*P* = 0.000, **Figure 1C**). Compared with the sham group, the Zea-longa scores of HIE rats increased over the 24 hour monitoring period after HIE surgery (*P* = 0.000, **Figure 1C**). Rats subjected to HIE scored an average of 2 points, with posturing and circling towards the injured side. These results were an indication of brain injury and deterioration of the rats' neurological function.

The number of single-nucleotide polymorphisms was increased in hypoxia-ischemia brain damage rats

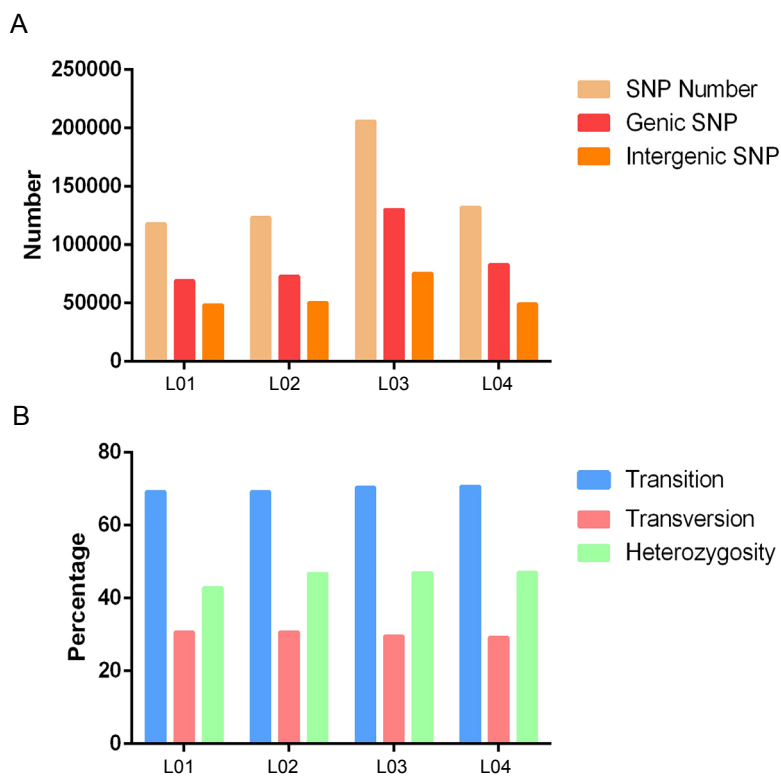
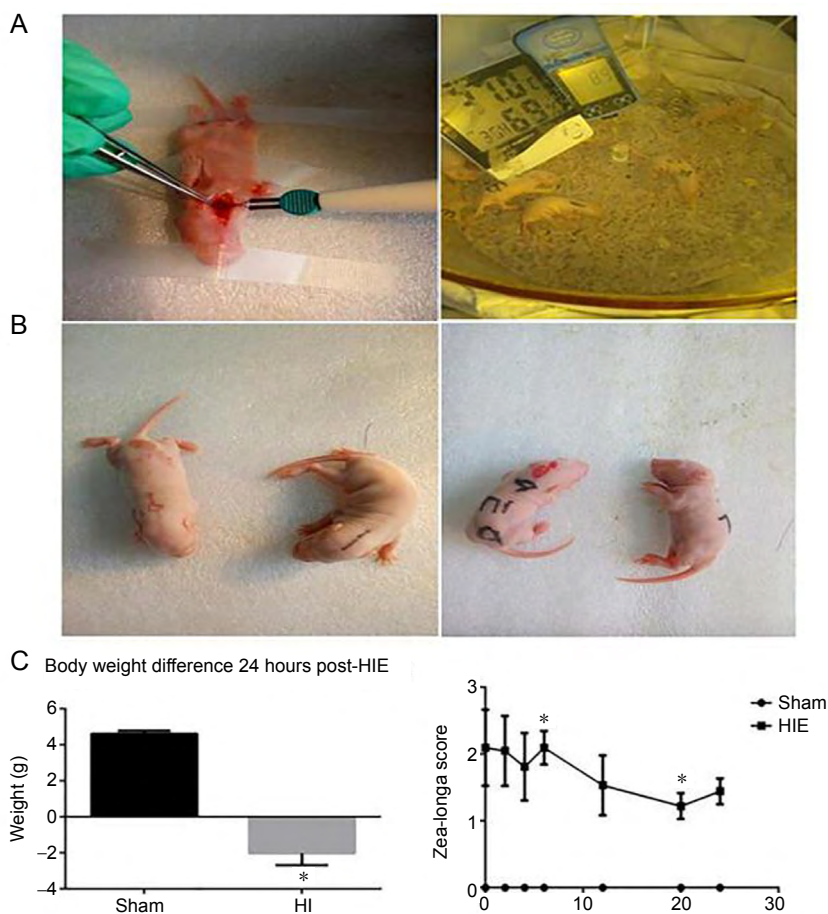
To confirm the correlation of HIE with particular SNPs, we compared the number of SNPs between HIE and sham groups (**Additional Table 1**). The SNP statistical analysis was based on comparison of the reads of each sample with reference genomes. There were 130248 and 83060 SNPs in the two HIE samples, with 75646 and 49372 SNPs in gene regions (**Figure 2A** and **Additional Table 1**). Meanwhile, the control group samples exhibited 69315 and 72933 SNPs in total, with 48728 and 50516 SNPs, respectively, in gene regions (**Figure 2A** and **Additional Table 1**). Evidently, the HIE group exhibited a higher total number of SNPs and a higher number of SNPs in gene regions. This indicated that HIE induced genomic SNPs; however, there were no differences of transition, transversion and heterozygosity of SNPs between the control and HIE groups (**Figure 2B**, **Additional Tables 1** and **2**).

Single-nucleotide polymorphism localization

The chromosomal location of SNPs was investigated in sham and HIE groups. The majority of detected SNPs were observed on the largest chromosomes (N1 and N2) as shown in **Additional Table 2**. Generally, the numbers of SNPs on each chromosome were higher in the HIE group compared with the control group.

SNP genotypes in the HIE group

To analyze distinct SNPs in the HIE group that might be involved in the etiology of HIE, we screened the SNPs according to genotype. A total of ten SNP genotypes were identified, including A, C, G, K, M, R, S, T, W, Y. The most common SNP genotype was G (3544) and the least common



was W (507) (Figure 3 and Additional Table 3).

Enrichment analysis for genes containing SNPs in HIE rats

Differentially expressed genes in both the sham and HIE groups were studied, as was enrichment analysis of GO data derived from sequence analysis. We detected 89 up-regulated genes, including *Csrnp1*, *Dusp5*, *Lrrc25*, *Cxcl1*, *Clca4l*, and *Serpine1* exhibiting SNPs in the HIE group compared with the sham group (Figure 4 and Additional Table 4). Compared with the sham group, HIE induced more genes to contain SNPs. These genes were involved in cell adhesion, peptidyl-serine phosphorylation, protein autophosphorylation, cytoplasm, cytosol, cell junction, axon, dendrite, dendritic spine, synapse, postsynaptic membrane, phospholipid binding, protein kinase binding, PDZ domain binding and protein complex binding. These functions were in addition to processes common with the sham group, including postsynaptic density, neuronal cell body and ATP binding with neuronal cell body (Figure 4A & B). In addition, pathway analysis revealed that only genes in the sham group containing SNPs were mainly involved in mitogen-activated protein kinase, sphingolipid, adrenergic signaling in cardiomyocytes, circadian entrainment, retrograde endocannabinoid and dopaminergic synapse pathways (Figure 4A). Meanwhile, up-regulated genes containing SNPs only in the HIE group, mainly participated in mitogen-activated protein kinase, circadian entrainment, retrograde endocannabinoid signaling, glutamatergic synapse, long-term depression and oxytocin

signaling pathways (Figure 4B). These were quite different from those of the sham group.

Further gene ontology analysis of the up-regulated genes containing SNPs in the HIE rats

The majority of mRNA targets in the HIE group were associated with 14 biological processes, including angiogenesis involved in wound healing, bone morphogenetic protein signaling pathway, cell adhesion, immune response, integrin-mediated signaling pathway, regulation of innate immune system, negative regulation of cytokine-mediated immunity, neutrophil chemotaxis, palate development and positive regulation of protein phosphorylation (Figure 5).

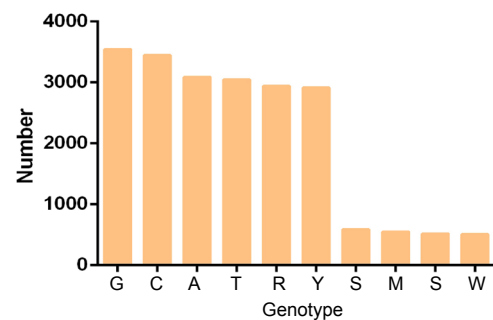


Figure 3 Numbers of SNPs in the ten genotypes of the HIE group. The abscissa represents the genotypes and the ordinate represents the number of each genotype. HIE: Hypoxic ischemic encephalopathy; SNPs: single-nucleotide polymorphisms.

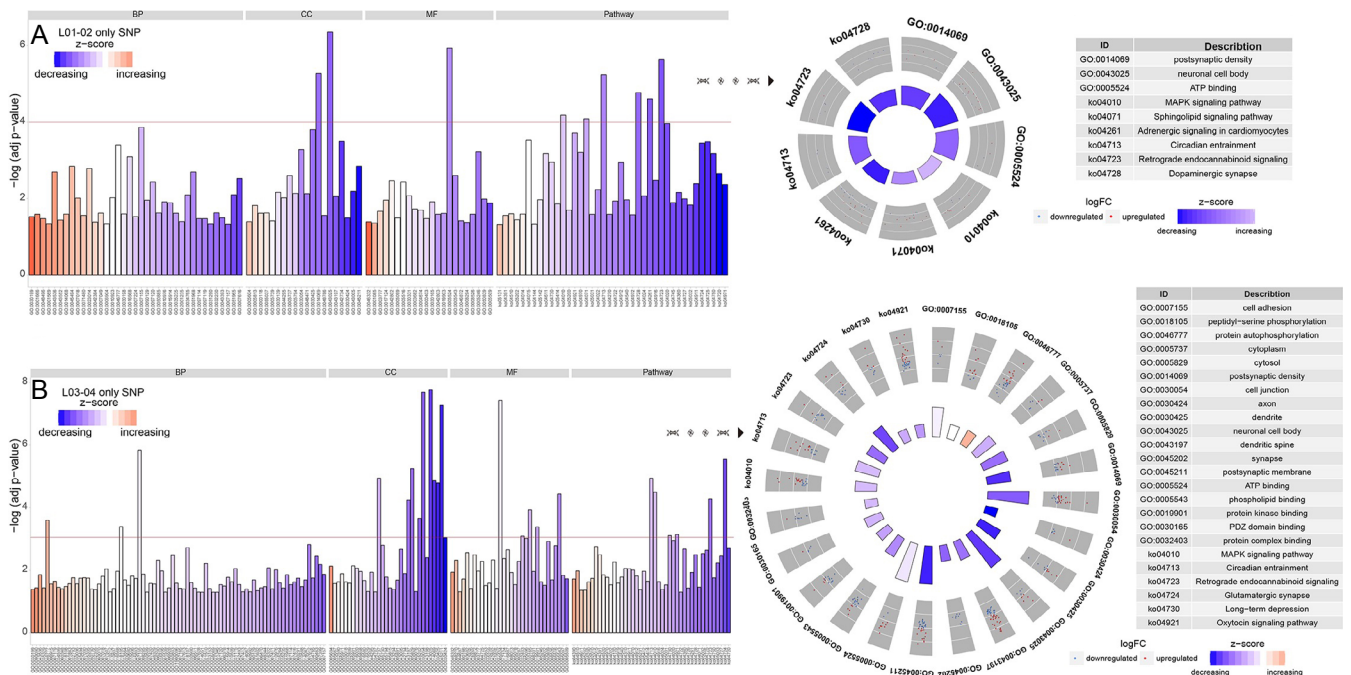


Figure 4 Enrichment analysis of GO terms for differentially expressed mRNAs.

The three most significant items of each GO term are listed in the bar chart. The horizontal axis shows the GO annotations and pathway, and the vertical axis shows the *P* value. (A) The GO analysis and pathway analysis of the differentially expressed genes in the sham group. Blue represents decreasing expression. Red represents increasing expression. The right chart shows the top nine differentially expressed genes. (B) The GO and pathway analysis of the differentially expressed genes in HIE group. Blue represents decreasing expression. Red represents increasing expression. The right chart shows the top 24 differentially expressed genes. BP: Biological processes; CC: cellular components; GO: gene ontology; MF: molecular functions.

The GO results concur with the molecular functions analysis because they indicated that genes primarily participating in growth factor activity were ligands for protein kinases, the intracellular calcium activated chloride channel and epigenetic regulator binding regions within DNA (Figure 5). Similarly, a cellular components analysis showed that these differentially expressed genes encode proteins localized on the external side of the plasma membrane, and with adhesion cellular components, and the integrin alpha9-beta1 complex (Figure 5).

Validation of candidate genes of interest

To further screen the gene sequencing data for genes that are truly involved in HIE, a high-throughput screening via PubMed searching was carried out. This revealed 27 factors that have not been studied in HIE (Additional Table 5). Intersection analysis of these 27 genes with the 89 up-regulated genes exhibiting SNPs using Venny 2.2 software (<http://bioinfogp.cnb.csic.es/tools/venny/index.html>), identified three genes, *CSRNP1*, *DUSP5* and *LRRC25*, that possessed SNPs (Figure 6A). Therefore, they were assessed in the following experiment. Human fetal cortical neurons were cultured, and OGD was employed to monitor HIE *in vitro*. Two hours after OGD, the neurons exhibited obvious damage, as indicated by broken cell bodies and axons (Figure 6B). Meanwhile, qRT-PCR showed that the expressional levels of *CSRNP1*, *DUSP5* and *LRRC25* were significantly up-regulated 24 hours post OGD, compared with the normal group (*CSRNP1*: $P = 0.000$; *DUSP5*: $P = 0.000$; *LRRC25*: $P = 0.000$; Figure 6C-E).

Discussion

In this study, we performed a comprehensive analysis of SNPs and mRNA expression in cortical samples from rats subjected to HIE and sham operation. RNA sequencing revealed that HIE induced SNPs in mRNAs, which were mainly from genes on chromosomes 1 and 2. Phenotype analysis indicated the SNPs were commonly associated with a G phenotype and scarcely with a W phenotype. In addition, a total of 89 up-regulated genes containing SNPs were found in the HIE group, and were mainly involved in angiogenesis, wound healing biological process and glutamatergic synapse. This is in addition to long-term depression signaling pathways, which were closely correlated with the pathogenesis of HIE. Moreover, intersection analysis identified *CSRNP1*, *DUSP5* and *LRRC25* as the most relevant to HIE (Figure 7). These genes were also up-regulated in human neurons after OGD, which may be related to the pathology of HIE; therefore, they may be new targets for HIE therapy.

HIE pathogenesis is correlated with SNPs detected by RNA sequencing

It is acknowledged that some SNPs are associated with specific disorders and are the main reason for differences in disease susceptibility. A variety of human diseases, including sickle-cell anemia, β -thalassemia and cystic fibrosis are correlated with SNPs (Ingram, 1956; Chang and Kan, 1979; Hamosh et al., 1992). Equally, the seriousness of the disease and the way our body reacts to therapies are also manifestations

of genetic variation. A single base variation in poly (ADP-ribose) Polymerase-1, for example, is connected with gastrointestinal tumors (Martín-Guerrero et al., 2017); the rs1495741 genetic variant and smoking are strongly associated with the risk of bladder cancer (Ma et al., 2016); and the aldehyde dehydrogenase 2 Glu504Lys SNP is a candidate risk factor for a wide range of chronic diseases, including cancer, cardiovascular disease, and late-onset Alzheimer's disease, linked to lifestyle factors such as alcohol consumption and the presence of other genetic variations (Zhao and Wang, 2015). In addition, accumulating evidence shows that lung injury is associated with genetic variations (Wang et al., 2010a; Trittmann et al., 2014, 2016; Cho et al., 2015; Liu et al., 2016). In the present study, a large number of SNPs in HIE rats were detected via RNA-seq, indicating that HIE-induced brain injury was associated with the SNPs. Moreover, further study found 89 genes exhibiting SNPs that were up-regulated after HIE.

Gene ontology analysis of the up-regulated genes containing SNPs

A bioinformatics analysis was performed to predict the potential functions of the differentially expressed mRNAs containing SNPs in HIE rats. GO analysis categorized genes functions according to biological process, cellular component, and molecular function. Kyoto encyclopedia of genes and genomes analysis clarified the potential signaling pathways that genes might participate in. Compared with the control group, 89 genes exhibiting SNPs were up-regulated in the brain from the HIE group. This indicated that the effect of HIE-induced brain injury was a complex multi-gene process. The inflammatory response, together with excitotoxic and oxidative responses, are major contributors to ischemic injury in both the immature and adult brain (Ruscher et al., 2013; Fernández-Tajes et al., 2014). Angiogenesis is an important process in the recovery of brain ischemia-induced injury (Zheng et al., 2018). In our study, the GO analysis revealed that SNP-containing genes that were up-regulated 24 hours after HIE were mainly enriched for GO terms associated with the angiogenesis, wound healing, negative regulation of cytokine-mediated signaling pathway and negative regulation of innate immune response. Therefore, together with previous studies, our results revealed that SNPs in mRNA may influence biological processes after HIE.

A molecular function analysis revealed that the 89 up-regulated genes containing SNPs were mainly involved in growth factor activity, protein kinase binding, transcription regulatory region DNA binding, and intracellular calcium-activated chloride channel activity. The human genome contains about 560 protein kinase genes, accounting for about 2% of all human genes (Manning et al., 2002). Furthermore, kinases regulate the majority of cellular pathways, especially those involved in mechanistic cellular signaling and signal transduction (Murphy et al., 2014; Evers and Murphy, 2016). This suggests that the up-regulated genes containing SNPs were also involved in growth factor activity, which is important for recovery from HIE.

HIE typically results in serious long-term sequelae, mainly because of damage caused to neurons or axons in the acute

phase (Busl and Greer, 2010; Shankaran et al., 2012). Therefore, long-term neurological deficits from HIE are partially caused by inhibited axon regrowth. In the current study, pathway analysis indicated that the 89 up-regulated genes containing SNPs were mainly enriched in glutamatergic synapse and long-term depression signaling pathways, indicating that SNPs in mRNAs also participated in pathways involved in long-term neurological function.

CSRNP1, DUSP5 and LRRC25 are potential targets for HIE therapy

To select the most relevant genes involved in HIE, we performed high-throughput screening by searching PubMed and we used PCR to verify candidates. We identified 27 genes that have not been studied in HIE. In addition, 89 up-regulated genes containing SNPs were found in the HIE group by RNA sequencing. We intersected the 27 factors from high-throughput screening and the 89 up-regulated genes exhibiting SNPs using Venny. Three genes, *CSRNP1*, *DUSP5* and *LRRC25* were identified. qRT-PCR showed that the relative expression of *CSRNP1*, *DUSP5* and *LRRC25* was up-regulated in OGD-treated human fetal cortical neurons group compared with the control group. These data indicate that the three genes are candidate targets for HIE therapy, and they will inform further research on HIE pathogenesis.

In conclusion, this study's findings indicate that HIE is accompanied with an increased number of SNPs, which often exhibited in G phenotype and rarely the W phenotype. Additionally, 89 up-regulated genes containing SNPs were involved in angiogenesis, wound healing, negative regulation of cytokine-mediated signaling pathway, negative regulation of innate immune response and palate development, which may contribute to the pathogenesis and biochemical characteristics of HIE in neonatal rats. Finally, *CSRNP1*, *DUSP5* and *LRRC25* were verified by high throughput screening as the most relevant genes containing SNPs to HIE. However, we did not investigate the influence of SNP overexpression or knockout on HIE in the current study. In spite of this, our results provide robust evidence for advancing the development of HIE therapy.

Acknowledgments: We gratefully acknowledge Professor Fei Liu from Institute of Neurological Disease, Department of Anesthesiology, Translational Neuroscience Center, West China Hospital, Sichuan University, Chengdu, Sichuan Province, China for the suggestion on the paper.

Author contributions: Research design: THW, LLXiong; model establishing, RNA-Seq and bioinformatics analysis: LLXiong, LLXue, MAH, JH, RZN, YXT, YX, JL; data analysis: LLXiong, LLXue, YYS; manuscript writing: LLXiong, LLXue; manuscript revising: THW, LLXiong, LLXue. All authors approved the final version of the paper.

Conflicts of interest: The authors declare that they have no conflict of interest.

Financial support: This study was supported by the program Innovative Research Team in Science and Technology in Yunnan Province, China (to THW); the National Natural Science Foundation of China, No. 81601074, Sichuan Provincial Scientific Foundation Grant of China, No. 2017SZ0145. All authors declared that the financial supports did not affect the paper's views and statistical analysis of the objective results of the research data and their reports.

Institutional review board statement: This animal study was approved on February 5, 2017 by the Animal Care and Use Committee of Kunming Medical University, Yunnan Province, China (approval No. kmmu2019038). Cerebral tissue collection from a human fetus was ap-

proved on September 30, 2015 by the Ethics Committee of Kunming Medical University, China (approval No. 2015-9).

Copyright license agreement: The Copyright License Agreement has been signed by all authors before publication.

Data sharing statement: Datasets analyzed during the current study are available from the corresponding author on reasonable request.

Plagiarism check: Checked twice by iThenticate.

Peer review: Externally peer reviewed.

Open access statement: This is an open access journal, and articles are distributed under the terms of the Creative Commons Attribution-Non-Commercial-ShareAlike 4.0 License, which allows others to remix, tweak, and build upon the work non-commercially, as long as appropriate credit is given and the new creations are licensed under the identical terms.

Additional files:

Additional Figure 1: The correlation analysis of linear regression among weight, Zea-longa score and the number of SNPs found that there is no significant difference between the weight and the number of SNPs as well as the Zea-longa score in HIE group.

Additional Table 1: The total number of single-nucleotide polymorphisms (SNPs) in sham and hypoxic ischemic encephalopathy (HIE) groups.

Additional Table 2: The number of single-nucleotide polymorphisms (SNPs) in all of samples.

Additional Table 3: The number of single-nucleotide polymorphisms (SNPs) in A, C, G, K, M, R, S, T, W, Y genotypes.

Additional Table 4: The upregulated genes in hypoxic ischemic encephalopathy (HIE) compared with the sham group.

Additional Table 5: Advances in genes research.

References

- Alaro D, Bashir A, Musoke R, Wanaiana L (2014) Prevalence and outcomes of acute kidney injury in term neonates with perinatal asphyxia. *Afr Health Sci* 14:682-688.
- Allen KA, Brandon DH (2011) Hypoxic ischemic encephalopathy: pathophysiology and experimental treatments. *Newborn Infant Nurs Rev* 11:125-133.
- Busl KM, Greer DM (2010) Hypoxic-ischemic brain injury: pathophysiology, neuropathology and mechanisms. *NeuroRehabilitation* 26:5-13.
- Chang JC, Kan YW (1979) beta 0 thalassemia, a nonsense mutation in man. *Proc Natl Acad Sci U S A* 76:2886-2889.
- Chau V, Poskitt KJ, Dunham CP, Hendson G, Miller SP (2014) Magnetic resonance imaging in the encephalopathic term newborn. *Curr Pediatr Rev* 10:28-36.
- Cho HY, Jedlicka AE, Gladwell W, Marzec J, McCaw ZR, Bienstock RJ, Kleeberger SR (2015) Association of Nrf2 polymorphism haplotypes with acute lung injury phenotypes in inbred strains of mice. *Antioxid Redox Signal* 22:325-338.
- Costantine MM, Clark EA, Lai Y, Rouse DJ, Spong CY, Mercer BM, Sorokin Y, Thorp JM, Jr., Ramin SM, Malone FD, Carpenter M, Miodovnik M, O'Sullivan MJ, Peaceman AM, Caritis SN (2012) Association of polymorphisms in neuroprotection and oxidative stress genes and neurodevelopmental outcomes after preterm birth. *Obstet Gynecol* 120:542-550.
- Davies A, Wassink G, Bennet L, Gunn AJ, Davidson JO (2019) Can we further optimize therapeutic hypothermia for hypoxic-ischemic encephalopathy? *Neural Regen Res* 14:1678-1683.
- Ding H, Zhang H, Ding H, Li D, Yi X, Ma X, Li R, Huang M, Ju X (2017) Transplantation of placenta-derived mesenchymal stem cells reduces hypoxic-ischemic brain damage in rats by ameliorating the inflammatory response. *Cell Mol Immunol* 14:693-701.
- Eyers PA, Murphy JM (2016) The evolving world of pseudoenzymes: proteins, prejudice and zombies. *BMC Biol* 14:98.
- Fernández-Tajes J, Soto-Hermida A, Vázquez-Mosquera ME, Cortés-Pereira E, Mosquera A, Fernández-Moreno M, Oreiro N, Fernández-López C, Fernández JL, Rego-Pérez I, Blanco FJ (2014) Genome-wide DNA methylation analysis of articular chondrocytes reveals a cluster of osteoarthritic patients. *Ann Rheum Dis* 73:668-677.
- Ginsberg MD (2008) Neuroprotection for ischemic stroke: past, present and future. *Neuropharmacology* 55:363-389.
- Goldstein JA (2001) Clinical relevance of genetic polymorphisms in the human CYP2C subfamily. *Br J Clin Pharmacol* 52:349-355.
- Graham EM, Ruis KA, Hartman AL, Northington FJ, Fox HE (2008) A systematic review of the role of intrapartum hypoxia-ischemia in the causation of neonatal encephalopathy. *Am J Obstet Gynecol* 199:587-595.
- Hamosh A, King TM, Rosenstein BJ, Corey M, Levison H, Durie P, Tsui LC, McIntosh I, Keston M, Brock DJ (1992) Cystic fibrosis patients bearing both the common missense mutation Gly---Asp at codon 551 and the delta F508 mutation are clinically indistinguishable from delta F508 homozygotes, except for decreased risk of meconium ileus. *Am J Hum Genet* 51:245-250.
- Ingolia NT, Brar GA, Rouskin S, McGeachy AM, Weissman JS (2012) The ribosome profiling strategy for monitoring translation in vivo by deep sequencing of ribosome-protected mRNA fragments. *Nat Protoc* 7:1534-1550.

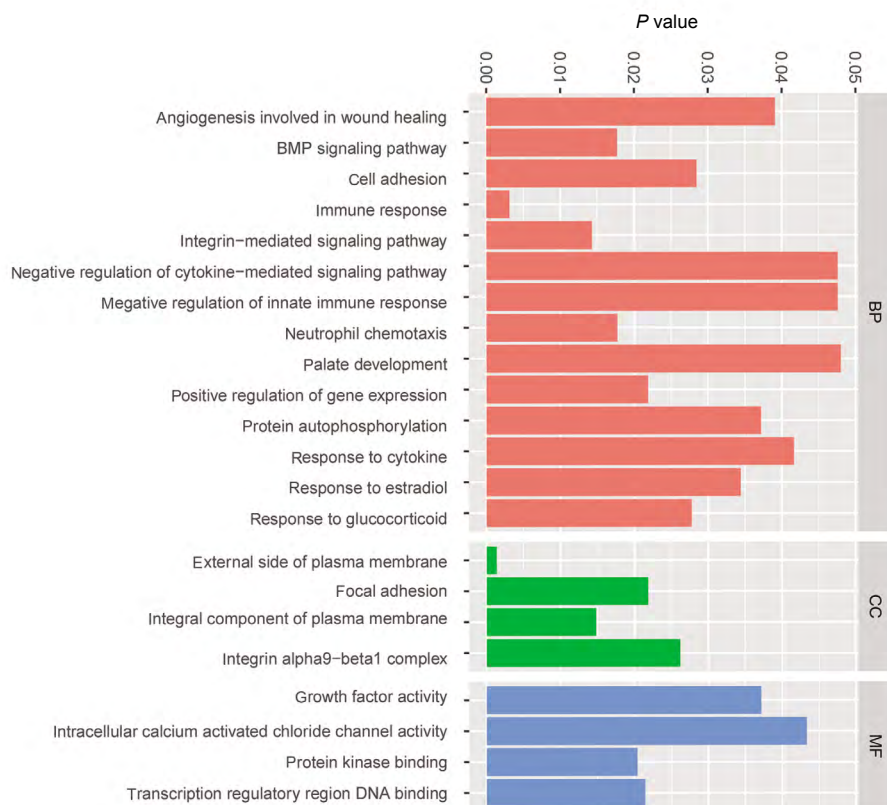


Figure 5 Gene ontology analysis of the genes containing SNPs.

A map of the 14 biological processes (BP), 4 cellular components (CC) and 4 molecular functions (MF) for the up-regulated genes containing SNPs after HIE. The vertical axis shows the P value. BMP: Bone morphogenetic protein.

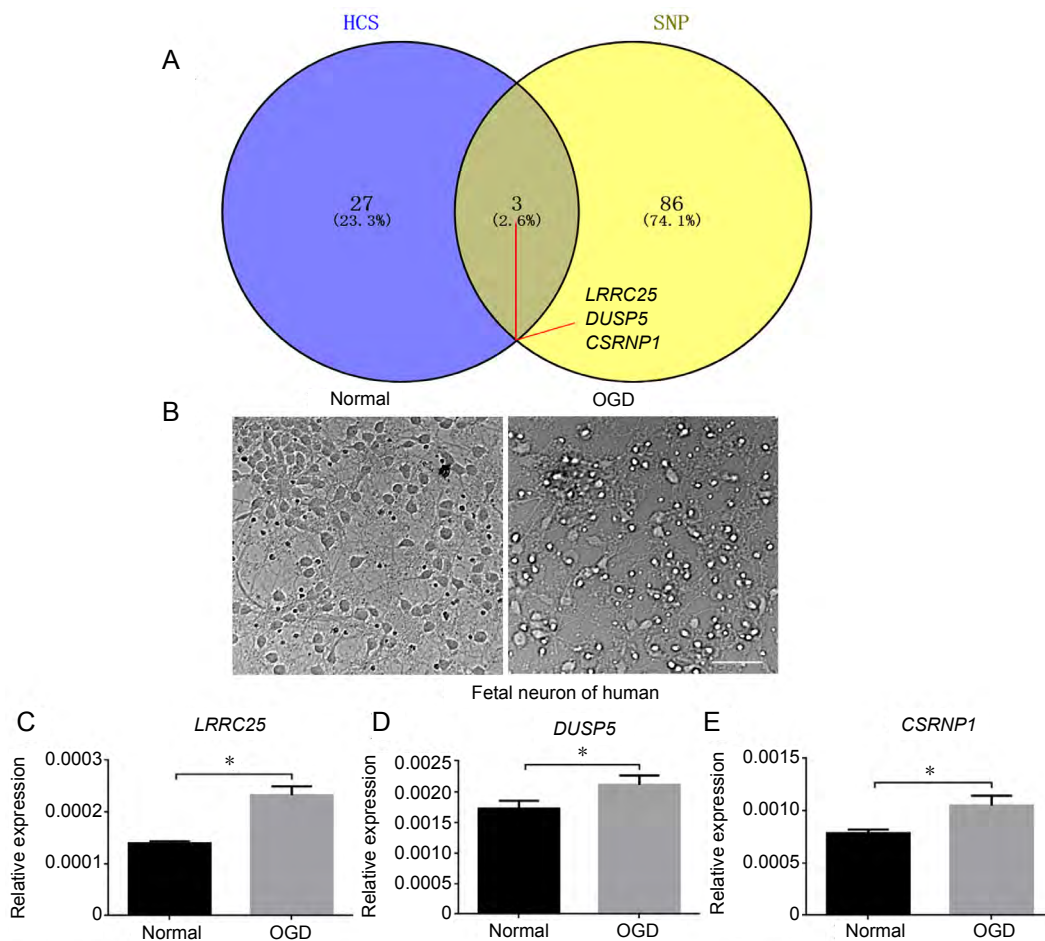


Figure 6 The validation of candidate genes of interest.

Screening for candidate genes by PubMed searching and SNP sequencing. (A) Three genes (*CSRNP1*, *DUSP5* and *LRRC25*) were identified by Venny 2.1 from 27 genes detected by HCS and 89 differentially up-regulated genes containing SNPs. (B) The morphology of fetal cortical neuron growth in normal and oxygen-glucose deprivation (OGD) groups. The red arrows indicate fetal neurons. Scale bar: 50 μm. (C-E) The relative expression ($2^{-\Delta\Delta C_t}$) of *CSRNP1*, *DUSP5* and *LRRC25* in normal and OGD groups at 24 hours post OGD. Data are expressed as the mean ± SD, and were analyzed by Student's *t* test. **P* < 0.05. HCS: High-throughput screening; SNP: single-nucleotide polymorphism.

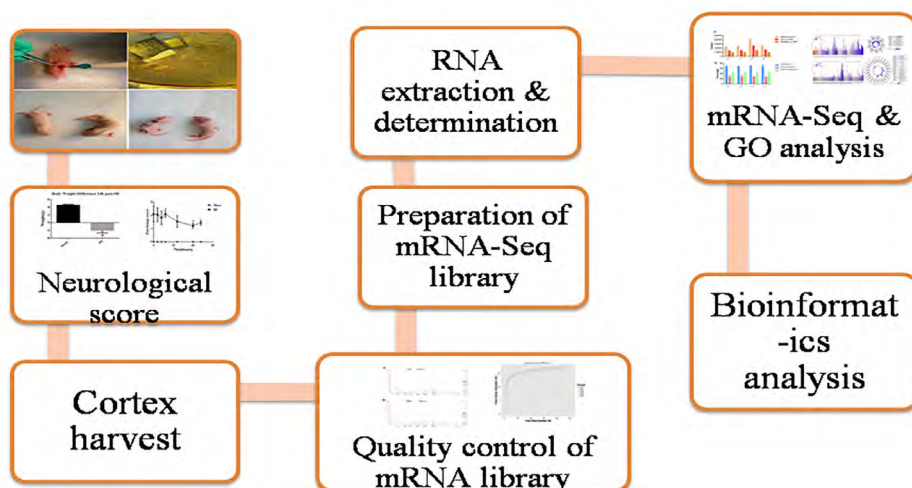


Figure 7 Flow chart of experimental strategy.

A hypoxic ischemic encephalopathy model was prepared and the neurological score of animals was determined. The cortex of each animal was extracted 24 hours post-operation. RNA was extracted and mRNA-sequencing (seq) libraries were prepared. After quality control of the mRNA library, mRNA-seq and gene ontology (GO) analysis were performed. Finally, bioinformatics analysis was conducted.

Ingram VM (1956) A specific chemical difference between the globins of normal human and sickle-cell anaemia haemoglobin. *Nature* 178:792-794.

Joergler-Messerli MS, Oppliger B, Spinelli M, Thomi G, di Salvo I, Schneider P, Schoeberlein A (2018) Extracellular vesicles derived from Wharton's jelly mesenchymal stem cells prevent and resolve programmed cell death mediated by perinatal hypoxia-ischemia in neuronal cells. *Cell Transplant* 27:168-180.

Khatri M, Himmelfarb J, Adams D, Becker K, Longstreth WT, Tirschwell DL (2014) Acute kidney injury is associated with increased hospital mortality after stroke. *J Stroke Cerebrovasc Dis* 23:25-30.

Lee CR (2004) CYP2C9 genotype as a predictor of drug disposition in humans. *Methods Find Exp Clin Pharmacol* 26:463-472.

Li G, Pan T, Guo D, Li LC (2014) Regulatory variants and disease: The E-cadherin -160C/A SNP as an example. *Mol Biol Int* 2014:967565.

Li PF, Wang T, Ma XL (2019) Association between COL9A2 gene polymorphisms and intervertebral disc degeneration in Asian: a meta-analysis. *Zhongguo Zuzhi Gongcheng Yanjiu* 23:3275-3280.

Liu B, Yi M, Tang Y, Liu Q, Qiu H, Zou Y, Peng P, Zhang L, Hu C, Yuan X (2016) MMP-1 promoter polymorphism is associated with risk of radiation-induced lung injury in lung cancer patients treated with radiotherapy. *Oncotarget* 7:70175-70184.

Liu R, Zhao W, Zhao Q, Liu SJ, Liu J, He M, Xu Y, Wang W, Liu W, Xia QJ, Li CY, Wang TH (2014) Endoplasmic reticulum protein 29 protects cortical neurons from apoptosis and promoting corticospinal tract regeneration to improve neural behavior via caspase and Erk signal in rats with spinal cord transection. *Mol Neurobiol* 50:1035-1048.

Lu YF, Mauger DM, Goldstein DB, Urban TJ, Weeks KM, Bradrick SS (2015) IFNL3 mRNA structure is remodeled by a functional non-coding polymorphism associated with hepatitis C virus clearance. *Sci Rep* 5:16037.

Lv HY, Wu SJ, Wang QL, Yang LH, Ren PS, Qiao BJ, Wang ZY, Li JH, Gu XL, Li LX (2017) Effect of erythropoietin combined with hypothermia on serum tau protein levels and neurodevelopmental outcome in neonates with hypoxic-ischemic encephalopathy. *Neural Regen Res* 12:1655-1663.

Ma C, Gu L, Yang M, Zhang Z, Zeng S, Song R, Xu C, Sun Y (2016) rs1495741 as a tag single nucleotide polymorphism of N-acetyltransferase 2 acetylator phenotype associates bladder cancer risk and interacts with smoking: A systematic review and meta-analysis. *Medicine (Baltimore)* 95:e4417.

Maher CA, Kumar-Sinha C, Cao X, Kalyana-Sundaram S, Han B, Jing X, Sam L, Barrette T, Palanisamy N, Chinnaiyan AM (2009) Transcriptome sequencing to detect gene fusions in cancer. *Nature* 458:97-101.

Manning G, Whyte DB, Martinez R, Hunter T, Sudarsanam S (2002) The protein kinase complement of the human genome. *Science* 298:1912-1934.

Mao R, Wang X, Spitznagel EL, Jr., Frelin LP, Ting JC, Ding H, Kim JW, Ruczinski I, Downey TJ, Pevsner J (2005) Primary and secondary transcriptional effects in the developing human Down syndrome brain and heart. *Genome Biol* 6:R107.

Martin-Guerrero SM, Josefa L, Quiles-Perez R, Belmonte L, Martin-Oliva D, Ruiz-Extremera A, Salmeron J, Muñoz-Gómez JA (2017) Expression and single nucleotide polymorphism of poly (ADPRibose) polymerase-1 in gastrointestinal tumours: clinical involvement. *Curr Med Chem* 24:2156-2173.

Murphy JM, Zhang Q, Young SN, Reese ML, Bailey FP, Eyers PA, Ungureanu D, Hammaren H, Silvennoinen O, Varghese LN, Chen K, Tripaydonis A, Jura N, Fukuda K, Qin J, Nimchuk Z, Mudgett MB, Elowe S, Gee CL, Liu L, et al. (2014) A robust methodology to subclassify pseudokinases based on their nucleotide-binding properties. *Biochem J* 457:323-334.

Rodríguez M, Silva J, López-Alfonso A, López-Muñoz MB, Peña C, Domínguez G, García JM, López-González A, Méndez M, Provencio M, García V, Bonilla F (2014) Different exosome cargo from plasma/bronchoalveolar lavage in non-small-cell lung cancer. *Genes Chromosomes Cancer* 53:713-724.

Ruscher K, Kuric E, Liu Y, Walter HL, Issazadeh-Navikas S, Englund E, Wieloch T (2013) Inhibition of CXCL12 signaling attenuates the posts ischemic immune response and improves functional recovery after stroke. *J Cereb Blood Flow Metab* 33:1225-1234.

Saeed F, Adil MM, Malik AA, Qureshi MH, Nahab F (2014) Worse in-hospital outcomes in patients with transient ischemic attack in association with acute kidney injury: analysis of nationwide in-patient sample. *Am J Nephrol* 40:258-262.

Seeliger C, Karpinski K, Haug AT, Vester H, Schmitt A, Bauer JS, van Griensven M (2014) Five freely circulating miRNAs and bone tissue miRNAs are associated with osteoporotic fractures. *J Bone Miner Res* 29:1718-1728.

Shankaran S, Barnes PD, Hintz SR, Laptook AR, Zaterka-Baxter KM, McDonald SA, Ehrenkranz RA, Walsh MC, Tyson JE, Donovan EF, Goldberg RN, Bara R, Das A, Finan NN, Sanchez PJ, Poindexter BB, Van Meurs KP, Carlo WA, Stoll BJ, Duara S, et al. (2012) Brain injury following trial of hypothermia for neonatal hypoxic-ischaemic encephalopathy. *Arch Dis Child Fetal Neonatal Ed* 97:F398-404.

Storey JD, Tibshirani R (2003) Statistical significance for genomewide studies. *Proc Natl Acad Sci U S A* 100:9440-9445.

Trapnell C, Williams BA, Pertea G, Mortazavi A, Kwan G, van Baren MJ, Salzberg SL, Wold BJ, Pachter L (2010) Transcript assembly and quantification by RNA-Seq reveals unannotated transcripts and isoform switching during cell differentiation. *Nat Biotechnol* 28:511-515.

Trittmann JK, Gastier-Foster JM, Zmuda EJ, Frick J, Rogers LK, Vieland VJ, Chicoine LG, Nelin LD (2016) A single nucleotide polymorphism in the dimethylarginine dimethylaminohydrolase gene is associated with lower risk of pulmonary hypertension in bronchopulmonary dysplasia. *Acta Paediatr* 105:e170-175.

Trittmann JK, Nelin LD, Zmuda EJ, Gastier-Foster JM, Chen B, Backes CH, Frick J, Vaynshtok P, Vieland VJ, Klebanoff MA (2014) Arginase I gene single-nucleotide polymorphism is associated with decreased risk of pulmonary hypertension in bronchopulmonary dysplasia. *Acta Paediatr* 103:e439-443.

Vannucci RC (2000) Hypoxic-ischemic encephalopathy. *Am J Perinatol* 17:113-120.

Wang JF, Bian JJ, Wan XJ, Zhu KM, Sun ZZ, Lu AD (2010a) Association between inflammatory genetic polymorphism and acute lung injury after cardiac surgery with cardiopulmonary bypass. *Med Sci Monit* 16:CR260-265.

Wang W, Xu J, Li L, Wang P, Ji X, Ai H, Zhang L, Li L (2010b) Neuroprotective effect of morroniside on focal cerebral ischemia in rats. *Brain Res Bull* 83:196-201.

Wang WT, Sun YM, Huang W, He B, Zhao YN, Chen YQ (2016) Genome-wide long non-coding RNA analysis identified circulating lncRNAs as novel non-invasive diagnostic biomarkers for gynecological disease. *Sci Rep* 6:23343.

Wu YH, Zhang X, Wang DH (2011) Role of asymmetric dimethylarginine in acute lung injury induced by cerebral ischemia/reperfusion injury in rats. *Nan Fang Yi Ke Da Xue Xue Bao* 31:1289-1294.

Yanase K, Tsukahara S, Mitsuhashi J, Sugimoto Y (2006) Functional SNPs of the breast cancer resistance protein-therapeutic effects and inhibitor development. *Cancer Lett* 234:73-80.

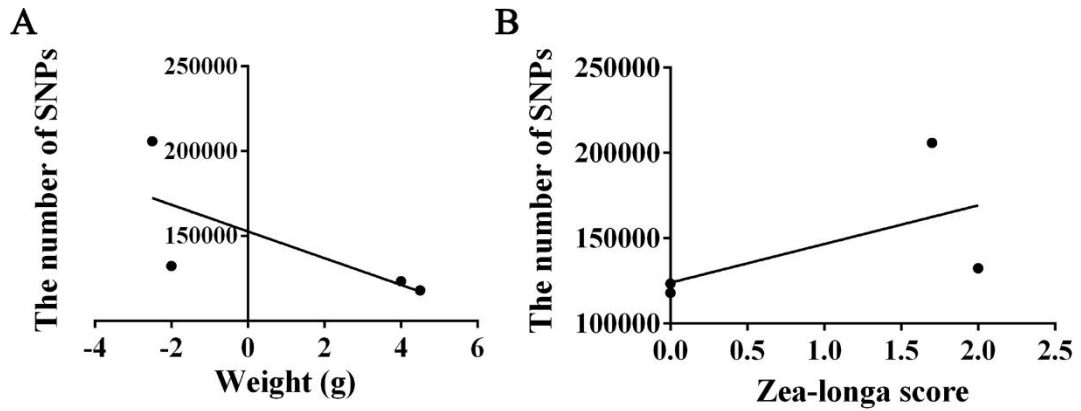
Zeppellini R, Salsa F, Gheno G, Cucchini F (2001) Cardiac injury in acute cerebral vasculopathy. *Ann Ital Med Int* 16:73-81.

Zhao S, Rong R, Dan QQ, Zhang YH (2012) Expression of trkB gene in the pulmonary tissue of rats with lung injury induced by cerebral ischemia. *Sichuan Da Xue Xue Bao Yi Xue Ban* 43:901-903, 958.

Zhao Y, Wang C (2015) Glu504Lys single nucleotide polymorphism of aldehyde dehydrogenase 2 gene and the risk of human diseases. *Biomed Res Int* 2015:174050.

Zheng Y, Wu Z, Yi F, Orange M, Yao M, Yang B, Liu J, Zhu H (2018) By activating Akt/eNOS bilobalide B inhibits autophagy and promotes angiogenesis following focal cerebral ischemia reperfusion. *Cell Physiol Biochem* 47:604-616.

C-Editor: Zhao M; S-Editors: Yu J, Li CH; L-Editors: Yu J, Song LP; T-Editor: Jia Y



Additional Figure 1 The correlation analysis among weight, Zea-longa score and the number of SNPs found that there is no significant difference between the weight and the number of SNPs as well as the Zea-longa score in HI group.

(A, B) Correlation linear analysis among the weight, Zea-longa score and the number of SNPs. Two points on the line represent sham group, the two points of dispersion represent HI group.

#Sample_ID	Snp_number_gene	Snp_number_intergenic	Transition (%)	Transversion (%)	Heterozygosity (%)	
L01	118043	69315	48728	69.31	30.69	42.81
L02	123449	72933	50516	69.25	30.75	46.77
L03	205894	130248	75646	70.40	29.60	47.05
L04	132432	83060	49372	70.77	29.23	47.10

L01 & L02 samples from control group; L03 & L04 samples from hypoxic ischemic encephalopathy group.

Gene ID	False Discovery rate	Log2FC (fold change)	Regulated	Gene name
gene10928	0.007321917	1.234849228	Up	<i>Cecr2</i>
gene11610	0.000494348	1.440158186	Up	<i>Chd7</i>
gene11832	0.000510142	1.401960952	Up	<i>B4galt1</i>
gene12406	0.036291268	1.405219558	Up	<i>Ror1</i>
gene12937	0.00059812	2.539193652	Up	<i>Fgr</i>
gene13033	0.017403119	1.11615355	Up	<i>LOC684122</i>
gene13264	8.00E-07	1.998225126	Up	<i>Casz1</i>
gene1410	0.006976111	1.195557824	Up	<i>Proser3</i>
gene14458	1.01E-08	1.517016795	Up	<i>Elmsan1</i>
gene15930	0.003616995	1.456447854	Up	<i>Irak3</i>
gene16622	1.82E-14	2.088731276	Up	<i>Ccdc134</i>
gene16625	0.001539985	1.275741357	Up	<i>Shisa8</i>
gene16799	1.04E-05	1.01371392	Up	<i>Ano6</i>
gene17912	0.014602678	1.127546269	Up	<i>Arid3b</i>
gene17977	0.033618102	1.652847862	Up	<i>Spesp1</i>
gene17997	0.001029297	1.770125454	Up	<i>Smad6</i>
gene18421	1.46E-05	2.000879142	Up	<i>Slco2a1</i>
gene18711	1.69E-05	1.280236316	Up	<i>Itga9</i>
gene18726	0.004030785	1.288195305	Up	<i>Xylb</i>
gene18736	1.23E-11	3.638238928	Up	<i>Csmp1</i>
gene18827	0.025594256	3.10825301	Up	<i>Ccr1</i>
gene19018	2.67E-16	Inf	Up	<i>LOC100912849</i>
gene19083	0.000139538	2.188379763	Up	<i>Runx2</i>
gene19085	0.030428257	1.484082283	Up	<i>Clic5</i>
gene20150	0.002857127	1.217668196	Up	<i>Vasn</i>
gene20655	0.019537489	1.38160466	Up	<i>Tcf7</i>
gene20938	0.000337032	2.83969408	Up	<i>Hs3st3b1</i>
gene21624	0.028824658	1.562356011	Up	<i>Pctp</i>
gene21784	0.000108425	2.220223383	Up	<i>Arl5c</i>
gene21921	2.95E-18	1.480593354	Up	<i>Stat3</i>
gene21922	6.95E-17	1.57894954	Up	<i>Ptrf</i>
gene22053	0.000267204	1.567816761	Up	<i>Itgb3</i>
gene22098	7.88E-09	1.368885314	Up	<i>Pecam1</i>
gene22145	0.007564055	1.691362364	Up	<i>Fam20a</i>
gene22728	5.87E-13	1.237620155	Up	<i>Ets2</i>
gene23174	0.000252217	2.317403614	Up	<i>Leprell1</i>
gene23185	0.001227681	1.037587703	Up	<i>Lpp</i>
gene23858	1.32E-46	5.16528331	Up	<i>Serpine1</i>
gene24177	0.011318539	1.216444191	Up	<i>Vsig10</i>
gene24687	3.47E-07	3.017963325	Up	<i>Ptprc</i>
gene25476	0.009700318	1.158533434	Up	<i>Tgfbr3</i>
gene25582	0.000392403	2.521693129	Up	<i>Fgf5</i>
gene25612	5.20E-08	1.768312007	Up	<i>Shroom3</i>
gene25643	1.44E-22	6.759783682	Up	<i>Cxcl1</i>
gene26603	1.77E-05	1.022215948	Up	<i>Flnb</i>
gene27014	0.004656377	1.004953379	Up	<i>Lats2</i>
gene27729	0.014227908	1.010355395	Up	<i>Dcp1a</i>
gene2782	0.001952483	1.028077146	Up	<i>Zfp143</i>
gene27887	0.035139802	3.219479213	Up	<i>Lrrc25</i>
gene28211	0.014214731	1.011538396	Up	<i>Pragmin</i>
gene28758	9.32E-05	1.426349769	Up	<i>Ror2</i>
gene28759	2.07E-15	1.516883601	Up	<i>Nfil3</i>
gene28852	1.67E-07	1.478320873	Up	<i>Rnf144b</i>
gene28867	7.98E-05	1.029774301	Up	<i>Rbm24</i>
gene28923	0.012709411	1.454983568	Up	<i>Mak</i>
gene28946	3.28E-06	1.664387255	Up	<i>Bmp6</i>
gene29280	1.94E-05	2.469452509	Up	<i>Sfrp4</i>

gene2954	0.01129745	1.184598231 Up	<i>Arhgap17</i>
gene29939	4.79E-05	1.17526293 Up	<i>Nrg2</i>
gene30479	1.26E-06	1.923075394 Up	<i>Zfp516</i>
gene3108	9.78E-09	2.654171021 Up	<i>Bag3</i>
gene31215	2.09E-06	1.651489706 Up	<i>Irf8</i>
gene31237	0.017930871	1.346726574 Up	<i>Zfp469</i>
gene31693	0.004789907	2.684390722 Up	<i>RT1-A1</i>
gene31715	0.002824524	1.266958747 Up	<i>Itpr3</i>
gene31863	6.56E-07	2.527943172 Up	<i>Itgb2</i>
gene31869	0.003597344	1.206319056 Up	<i>Coll8a1</i>
gene32290	0.013296976	1.495250541 Up	<i>Aim1</i>
gene33491	0.000675436	1.245128971 Up	<i>Lonrf3</i>
gene4319	7.61E-14	3.35208246 Up	<i>Dusp5</i>
gene4981	0.031396721	1.007595524 Up	<i>Fam105a</i>
gene5150	4.11E-06	1.815866502 Up	<i>Cp</i>
gene5422	1.93E-07	1.32403003 Up	<i>Wwtr1</i>
gene5687	7.30E-35	Inf Up	<i>Sh2d2a</i>
gene6379	5.43E-07	2.585755151 Up	<i>Synpo2</i>
gene6410	0.003597344	1.301344945 Up	<i>Zgrf1</i>
gene6465	0.005514585	1.771361524 Up	<i>Dkk2</i>
gene6493	0.031604667	1.320650436 Up	<i>Tacr3</i>
gene6563	0.02891601	1.643902108 Up	<i>Gbp5</i>
gene6564	0.000229551	2.077167857 Up	<i>LOC685067</i>
gene6587	7.44E-05	6.178383959 Up	<i>Clca4l</i>
gene7067	0.029239889	1.105943242 Up	<i>Ptgs1</i>
gene7238	4.90E-11	1.174738611 Up	<i>gene7238</i>
gene8116	2.92E-52	3.079275962 Up	<i>Cd44</i>
gene9608	1.17E-08	1.836606238 Up	<i>Cdk6</i>
gene9626	0.020857722	3.432909322 Up	<i>Tfpi2</i>
gene9721	1.10E-06	1.640092399 Up	<i>Mdfic</i>
gene9738	0.00386661	2.268566993 Up	<i>Cftr</i>
gene9891	7.54E-13	1.752861704 Up	<i>Cald1</i>

Gene name	Synonyms	Description	GeneSummary	Transcription quantity	Sequence ID	Cellular localization	Literature quantity from Pubmed	Novoseek disease relationships for the gene	MalaCards disease relationships for the gene	Symbol	Number	False discovery rate	Fold change	Regulated	Function
3437	<i>IFIT3</i>	CIG-49 GARG-49 IF160 IFIT4 IRG2 SG60 P60 RIG-G	Interferon-induced protein with tetratricopeptide repeats 3	4	NM_001031683(1473), NM_001289759(1317), NM_001549(1473), NM_001289758(1317)	Cytoplasm. Mitochondrion	42	0	2	Ifit3	gene4056	1.83E-10	5.8044	Up	Negative regulation of cell proliferation
59271	<i>EVA1C</i>	B18 B19 C21orf63 C21orf64 FAM176C PRED34 SUE21	Eva-1 homolog C (<i>C. elegans</i>)	2	NM_001286556(1317), NM_058187(1326)	Membrane; Single-pass type I membrane protein (Potential)	10	0	0	Eva1c	gene22665	5.12E-11	4.2549	Up	Plasma membrane, integral component of membrane, carbohydrate binding
51804	<i>SIX4</i>	AREC3	SIX homeobox 4	1	NM_017420(2346)	Nucleus (By similarity)	18	0	0	Six4	gene14292	7.99E-09	4.2156	Up	Regulation of synaptic growth at neuromuscular junction, regulation of protein localization
10361	<i>NPM2</i>	-	Nucleophosmin/nucleoplasmin 2	3	NM_001286681(411), NM_182795(645), NM_001286680(645)	Nucleus (By similarity). Note=Found in the oocyte nucleus before nuclear membrane breakdown, after which it is redistributed to the cytoplasm (By similarity)	13	0	0	Npm2	gene27231	0.0000146	4.1234	Up	
115265	<i>DDIT4L</i>	REDD2 Rtp801L	DNA-damage-inducible protein 4	1	NM_145244(582)	Cytoplasm (By similarity)	14	0	1	Ddit4l	gene6516	5.36E-10	3.8915	Up	
64651	<i>CSRNP1</i>	AAUD1 CSRNP1 EAM120B TAD1	Cysteine-rich nuclear protein that localizes to the nucleolus	1	NM_033027(1770)	Nucleus (By similarity)	15	0	0	Csrnp1	gene18736	1.23E-11	3.6382	Up	
10981	<i>RAB32</i>	-	RAB32, member RAS oncogene family	1	NM_006834(678)	Mitochondrion. Cytoplasmic vesicle, phagosome. Cytoplasmic vesicle, phagosome membrane; Lipid-anchor; Cytoplasmic side (By similarity). Note=Recruited to phagosomes containing <i>S.aureus</i> or <i>M.tuberculosis</i> Explore the universe of human proteins at neXtProt for RAB32: NX_Q13637 Post-translational modifications:	19	0	0	Rab32	gene46	4.88E-28	3.4791	Up	
2634	<i>GBP2</i>	-	Guanylate binding protein 2, interferon gamma inducible	1	NM_004120(1776)	Cytoplasm. Nucleus. Golgi apparatus membrane; Lipid-anchor	31	0	0	Gbp2	gene6566	0.0000554	3.4162	Up	
1847	<i>DUSP5</i>	DUSP HVH3	Dual specificity phosphatase 5	1	NM_004419(1155)	Nucleus (Potential)	58	4	1	Dusp5	gene4319	7.61E-14	3.3521	Up	
126364	<i>LRRC25</i>	MAPA	Leucine rich repeat containing 25	1	NM_145256(918)	Membrane; Single-pass type I membrane protein (Potential)	8	0	0	Lrrc25	gene27887	0.0351398	3.2195	Up	
8638	<i>OASL</i>	OASL1 TRIP-14 TRIP14 p59 OASL p59-OASL p59OASL	Oligoadenylate synthetase-like	3	NM_001261825(1155), NM_198213(768), NM_003733(1545)	Isoform p56: Nucleus, nucleolus. Cytoplasm Isoform p30: Cytoplasm	39	0	0	Oasl	gene24225	0.0000296	3.2178	Up	
57820	<i>CCNB1IP1</i>	C14orf18 HEI10	Cyclin B1 interacting protein 1, E3 ubiquitin protein ligase	3	NM_182852(834), NM_021178(834), NM_182849(834)	Nucleus. Chromosome. Note=May associate with segregating chromosomes during metaphase and anaphase Explore the universe of human proteins at neXtProt for CCNB1IP1: NX_Q9NPC3 Post-translational modifications:	21	0	0	Ccnb1ip1	gene26728	0.0000691	3.1892	Up	
56833	<i>SLAMF8</i>	BLAME CD333 SDD1 17	SLAMF family class B member 8	1	NM_020125(858)	Membrane; Single-pass type I membrane protein	10	0	0	Slamf8	gene25120	7.95E-09	3.0308	Up	
79094	<i>CHAC1</i>	-	glutathione-specific gamma-SAM domain, SH3 domain and nuclear localization signals 1	2	NM_024111(795), NM_001142776(660)	Golgi apparatus, trans-Golgi network (By similarity). Cytoplasm, cytosol	14	0	0	Chac1	gene8349	7.27E-12	2.9496	Up	
64092	<i>SAMSN1</i>	HACS1 NASH1 SASH2 SH3D6B SLy2	SAMSN1 is a member of a novel gene family of putative adaptors and scaffold proteins	3	NM_001256370(1326), NM_022136(1122), NM_001286523(915)	Nucleus. Cytoplasm (By similarity). Cell projection, ruffle (By similarity). Note=Shuttles between cytoplasm and nucleus. Colocalizes with the actin cytoskeleton and actin-rich membrane ruffles (By similarity)	19	0	0	Samsn1	gene22523	0.0006012	2.8449	Up	
2615	<i>LRRC32</i>	D11S833E GARP	Leucine rich repeat containing 32	2	NM_001128922(1989), NM_005512(1989)	Membrane; Single-pass type I membrane protein	26	0	0	Lrrc32	gene2350	0.000000131	2.7125	Up	

55647	RAB20	-	RAB20, member RAS oncogene family	1	NM_017817(705)	Golgi apparatus. Cytoplasmic vesicle, phagosome. Cytoplasmic vesicle, phagosome membrane; Lipid-anchor; Cytoplasmic side (By similarity). Note=Highly enriched on apical endocytic structures in polarized epithelial cells of kidney proximal tubules (By similarity). Recruited to phagosomes containing S.aureus or M.tuberculosis	11	0	0	Rab20	gene28479	0.000000736	2.7008	Up
387496	RASL11A	-	RAS-like, family 11, member A	1	NM_206827(729)	Nucleus, nucleolus (By similarity). Note=Associates with rDNA transcription unit throughout the cell cycle (By similarity)	10	0	0	Rasl11a	gene23588	7.73E-10	2.6636	Up
55303	GIMAP4	LIAN-11A N1UMAD4 MSTD	GTPase, LMAP family member	1	NM_018326(990)	Cytoplasm, cytosol (By similarity)	17	0	1	Gimap4	gene10131	0.0055691	2.6318	Up
10457	GPNMB	HGFIN NMB	Glycoprotein (transmembrane) nmb	2	NM_002510(1683), NM_001005340(1719)	Membrane; Single-pass type I membrane protein (Potential). Melanosome. Note=Identified by mass spectrometry in melanosome fractions from stage I to stage IV	48	3	2	Gpnmb	gene10145	2.82E-20	2.594	Up
121549	ASCL4	HASH4 bHLHa44	Acute-scute family, HLH domain	1	NM_203436(522)	Nucleus (By similarity)	8	0	0	Ascl4	gene15593	0.0009807	2.5786	Up
55008	HERC6	-	HERC domain containing F2	2	NM_017912(3069), NM_001165136(2961)	Cytoplasm, cytosol	13	0	0	Herc6	gene10306	0.0044702	2.5675	Up
131450	CD200R1	CD200R HCRTR2 MOX2R OX2R	CD200 receptor 1	4	NM_138939(567), NM_170780(978), NM_138940(498), NM_138806(1047)	Isoform 1: Cell membrane; Single-pass type I membrane protein Isoform 4: Cell membrane; Single-pass type I membrane protein Isoform 2: Secreted Isoform 3: Secreted	46	0	0	Cd200r1	gene22955	0.0018284	2.4729	Up
51166	AADAT	KAT2 KATII	Aminoadipate aminotransferase	4	NM_016228(1278), NM_182662(1278), NM_001286683(1278), NM_001286682(1290)	Mitochondrion (Potential)	32	0	1	Aadat	gene28019	0.0042495	2.4221	Up
23704	KCNE4	MIRP3	Potassium channel subunit	1	NM_080671(666)	Membrane; Single-pass type I membrane protein	26	0	0	Kcne4	gene19690	0.0239597	2.4019	Up
54626	HES2	bHLHb40	Basic helix-loop-helix	1	NM_019089(522)	Nucleus (By similarity)	8	0	0	Hes2	gene13331	0.0025872	2.3469	Up
84617	TUBB6	HsT1601 TUBB-5	Tubulin, beta 6 class V	8	NM_001303526(1230), NM_032525(1341), NM_001303530(903), NM_001303527(1125), NM_001303528(1146), NM_001303529(903), NM_001303524(1341), NM_001303525(315)	Cytoplasm, cytoskeleton (By similarity)	45	0	1	Tubb6	gene30325	2.86E-30	2.3358	Up
152007	GLIPR2	C9orf19 GAPR-1 GAPR1	GLI pathogenesis-related 2	6	NM_022343(465), NM_001287014(219), NM_001287010(387), NM_001287013(510), NM_001287012(189), NM_001287011(315)	Golgi apparatus membrane; Lipid-anchor. Note=Binds lipid-enriched microdomains of Golgi membranes not only by ionic interactions but also through the myristate	22	0	0	Glipr2	gene11917	4.52E-08	2.2159	Up
91543	RSAD2	2510004L01Rik cig33 cig5 vig1	Radical S-adenosyl methionine domain containing 2	1	NM_080657(1086)	Endoplasmic reticulum membrane; Peripheral membrane protein; Cytoplasmic side. Golgi apparatus. Endoplasmic reticulum. Lipid droplet (By similarity). Mitochondrion. Mitochondrion inner membrane. Mitochondrion outer membrane. Note=Infection with human cytomegalovirus (HCMV) causes relocation to the Golgi apparatus and to cytoplasmic vacuoles which also contain HCMV proteins glycoprotein B and pp28. Interaction with human cytomegalovirus/HHV-5 protein vMIA/UL37 results in its relocalization from the endoplasmic reticulum to the mitochondria	45	0	0	Rsad2	gene13889	0.000000123	2.1947	Up
8676	STX11	FHL4 HLH4 HPLH4	Syntaxin 11	1	NM_003764(864)	Membrane; Peripheral membrane protein (Potential). Golgi apparatus, trans-Golgi network membrane; Peripheral membrane protein (By similarity)	44	0	5	Stx11	gene63	0.0000149	2.153	Up